

Threshold Alignment Reversal and Circularly Polarized Fluorescence in Rotationally Resolved H₂

J. W. Maseberg,^{1,2} K. Bartschat,³ and T. J. Gay¹

¹*Department of Physics and Astronomy, University of Nebraska, Lincoln, Nebraska 68588-0299, USA*

²*Department of Physics, Fort Hays State University, Hays, Kansas 67601-4099, USA*

³*Department of Physics and Astronomy, Drake University, Des Moines, Iowa 50311-4505, USA*

(Received 26 August 2013; published 17 December 2013)

Using H₂ and D₂ targets, we have measured the polarization of Fulcher-band fluorescence resulting from spin-polarized electron-impact excitation of vibrationally and rotationally resolved $d^3\Pi_u \rightarrow a^3\Sigma_g^+$ transitions for incident electron energies from 14.3 to 28.5 eV. Near threshold, the linear polarization P_1 descends from positive values through zero to negative values, indicating a dynamic production of $M_N = 0$ states. The circular polarization P_3 is measured to be nonzero, indicating the orientation of rotationally resolved molecular states. For Q -branch transitions, P_3 is consistent with theory based on Hund's case (b) coupling. The R -branch P_3 values do not agree with theory equally well, indicating the effect of Σ -symmetry perturbation of the parent $d^3\Pi_u^+$ state.

DOI: [10.1103/PhysRevLett.111.253201](https://doi.org/10.1103/PhysRevLett.111.253201)

PACS numbers: 34.80.Gs, 34.80.Nz

Experiments studying electron-impact excitation of atoms and molecules, such as the Franck-Hertz experiment [1], played a crucial role in the early development of the quantum theory. As experiments became more sophisticated, well-defined beams of electrons with precisely known energies striking targets in single-collision conditions yielded ever-more detailed information about the many-body collision dynamics of electron-impact excitation and/or fragmentation. Today's sophisticated experiments, involving various combinations of high energy resolution, multiple particle detection, fluorescence and particle polarization analysis, and spin-polarized constituents, can provide highly detailed information about individual collisions [2,3]. Experiments have advanced in step with improvement to both computational and analytical theory to the point where it is reasonable to assert that electron scattering from quasi-one- and quasi-two-electron atoms is essentially a solved problem. The same cannot be said for molecules; benchmark measurements and accompanying theory for electron impact excitation of simple systems with well-defined quantum numbers are almost nonexistent [2,3].

An ongoing question in studies of electron-impact excitation of atoms has been the nature of the excited atomic states just above the energy threshold for their production. This is an important problem, because it involves slowly separating collision partners where strong Coulombic coupling of multiple particles occurs for an extended period of time. Conservation laws place rigorous restrictions on the states that can be excited just above threshold; essentially, the momentum transfer from the incident electron to the atomic system must be purely longitudinal [4]. Thus, in the case of a one-electron excitation process, the initial electron momentum must be transferred completely to the excited electron's orbital [see Fig. 1(a)]. Consider, for

example, an $S \rightarrow P$ transition with the z -quantization axis taken along the incident beam direction. Ignoring spin and arguing classically, this means that only states with $M_L = 0$ can be excited, because the $M_L = \pm 1$ states have no longitudinal momentum. Quantum mechanically, this corresponds to the excitation of a p_z orbital. Upon decay to the ground state, the fluorescence must thus be linearly polarized along the z axis, with the linear polarization fraction $P_1 = (I_{\parallel} - I_{\perp}) / (I_{\parallel} + I_{\perp}) = +1$, where I_{\parallel} (I_{\perp}) is the intensity of the fluorescence polarized parallel (perpendicular) to the z axis [5]. Generally, the value of +1 is reduced by a number of kinematic factors internal to the target: electron spin and nuclear spin depolarization and the atomic orbital angular momentum coupling scheme [4–6]. Certain coupling schemes can lead to negative values of P_1 [7–9]. In all cases, however, threshold dynamics rigorously require that only states with $M_L = 0$ be populated at threshold. Very early measurements of fluorescence polarization from electron-beam excitation of Hg by Skinner and Appleyard showed that this picture is incomplete [8]. Failure of their data to match the kinematically required threshold values called into question the new quantum theory and occasioned much theoretical work to explain their anomalous results [4,6,10]. Indeed, it was not until the late 1960s that a reasonably comprehensive understanding of such anomalous threshold values emerged. While the correct kinematic limit is required by quantum mechanics, this restriction holds only as the excess energy above threshold goes to zero. Essentially all extant anomalous results can be understood in terms of inadequate experimental energy resolution, near-threshold temporary negative-ion resonances, or both [9–12].

In the case of molecular targets, the situation is very different. There exists, to our knowledge, only one previous study of threshold polarization for well-defined

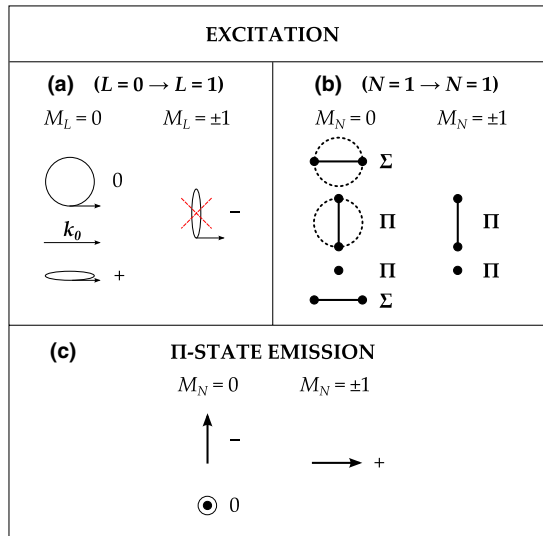


FIG. 1 (color online). The classical dynamics of threshold excitation for both atoms and molecules (see text). (a) $S \rightarrow P$ atomic excitation showing the P -state M_L orbitals. The direction of the incident electron momentum k_0 , which is the same as the momentum transfer at threshold, is indicated. The 0, +, and - signs indicate the sign of P_1 produced when the respective M_L states decay. (b) $\Sigma \rightarrow \Sigma$ or $\Sigma \rightarrow \Pi$ molecular excitation for $N = 1$. Various nuclear rotational orientations at a given instant are shown, with the electronic state that can be excited for purely longitudinal momentum transfer. The dashed circles represent the nuclear orbitals over time. Unlike the atomic threshold case, molecular Π -state excitation can yield $M_N = \pm 1$ and 0. (c) Signs of P_1 for Π -state emission. The arrows indicate the classical direction of N .

excited states [13]. In this Letter, we present systematic measurements of fluorescence polarization from rotationally and vibrationally resolved states of the fundamental H_2 system. By using an incident spin-polarized electron beam, we have succeeded in observing orientation induced by electron impact of target molecular states whose angular momentum quantum numbers are completely known. These data match well with our theoretical predictions for a pure Hund's case (b) coupling of three angular momenta. We also find that with molecules the linear polarization can have a negative limit at threshold due not to kinematic target coupling but to the direct dynamic excitation of $M_N = 0$ states.

The experimental apparatus we used to perform these measurements is shown in Fig. 2 of Ref. [14], and a detailed discussion of our basic experimental procedure is given there. Briefly, we obtain a beam of transversely spin-polarized electrons by irradiating unstrained negative electron affinity (NEA) GaAs with circularly polarized 785 nm laser light. Photoelectrons from this source have an energy width of less than 0.4 eV and a polarization $P_e \approx 27\%$. A differential pumping region separates the source from the field-free target gas cell, whose potential is varied to change the collision energy. A lens above the target cell

images light from excited molecules into an optical polarimeter, comprising a rotatable quarter-wave retarder, linear polarizer, optical bandpass filter, and a cooled Hamamatsu R946 photomultiplier tube. We use individual, very narrow (0.14 nm FWHM) interference filters for wavelengths 600.7, 601.8, 618.3 nm, 622.5, and 623.8 nm, to isolate each of the molecular rotational transitions of interest: $D_2 Q(3)[0]$, $H_2 Q(1)[0]$, $H_2 R(1)[2]$, $H_2 Q(1)[2]$, and $H_2 Q(3)[2]$, respectively, where the number in square brackets is both the excited-state and final-state vibrational quantum number. In the $Q(N)$ transitions, the initial, excited, and final states have nuclear rotational quantum number N . In all cases, the total nuclear spin is $I = 1$. These transitions were picked to be well separated from other, spectrally dense transitions of the Fulcher band.

Our data are shown in Figs. 2 and 3. Figure 2 focuses on P_1 for the $H_2 Q(1)$ transitions, for which there exist other theoretical and experimental data for comparison. Figure 3 shows all of our polarization data, including those for the circular polarization fraction P_3 , which is proportional to the electron spin-induced magnetic dipole moment of the excited molecular states [5].

We comment first on some general features of the data. Our P_1 results displayed in Fig. 2, while in qualitative agreement with previous experimental values [13,15,16], are in qualitative disagreement with theory [17]. Our data in Figs. 2 and 3 decrease monotonically toward zero as the threshold energy is approached, and some transitions reach negative values for the lowest energies. In addition to the data of Ref. [13] and that for rotationally unresolved transitions in N_2 [18,19], these are the only data of which we are aware that exhibit this behavior, with the caveats that the collisions involve simple excitation without fragmentation and are unperturbed by the presence of obvious negative-ion resonances. We note that a few atomic systems [7,9,20] exhibit this behavior, but do so as required by

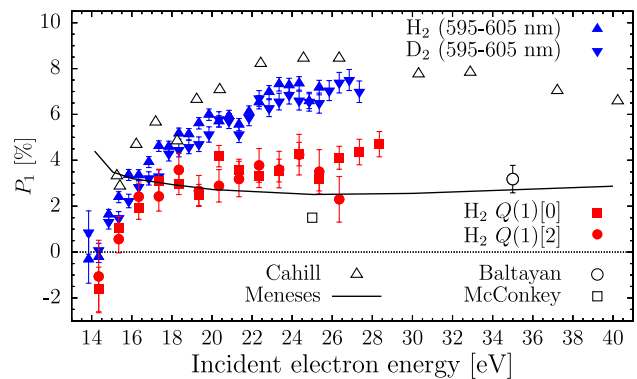


FIG. 2 (color online). Linear polarization fraction P_1 as a function of incident electron energy for excitation of the $Q(1)$ transition. The present rotationally resolved results are compared with our previous measurements with a wider bandwidth filter [18] and data from other groups [13,15,16]. Also shown are the theoretical predictions of Meneses *et al.* [17].

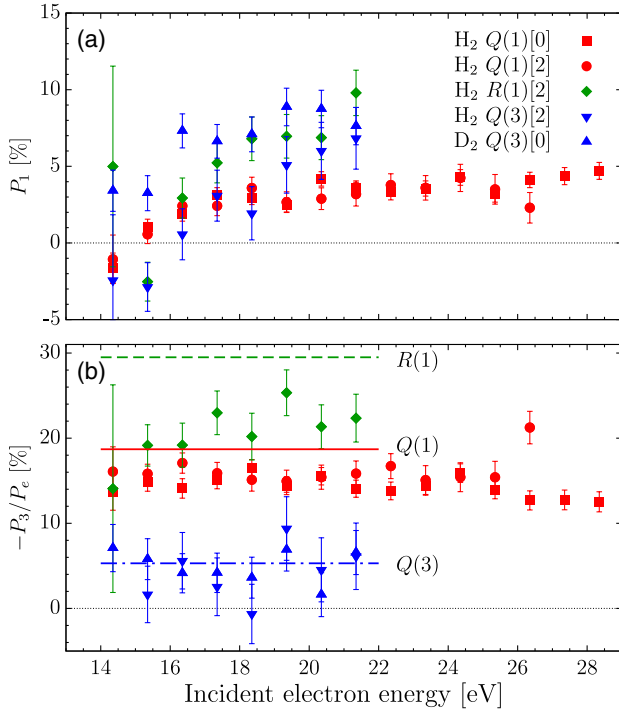


FIG. 3 (color online). (a) Linear polarization fraction P_1 for various transitions within the $H_2 d^3\Pi_u \rightarrow a^3\Sigma_g^+$ emission band. (b) The corresponding values of the circular light polarization P_3 . The latter are normalized to the incident electron polarization. The straight lines correspond to the values predicted in Eqs. (12)–(14).

target coupling kinematics and/or in the presence of strong resonances. While it is possible that our results are affected by rovibrational f -band resonances in the vicinity of 14–15 eV [21], we see no evidence for such features in our excitation functions or in the energy dependence of P_1 or P_3 . The behavior of P_1 is featureless from threshold to 28.5 eV, well above the range of such resonances. Moreover, we could find no reports for decay of these resonances into $d^3\Pi_u v = 0$ or 2 states; their major decay channels appear to be into $C^1\Pi_u$ and $c^3\Pi_u$ states [21].

In considering just our rotationally resolved P_1 data in both Figs. 2 and 3(a), it is apparent that, with the exception of the D_2 results, they reach negative values for energies closest to threshold. The data of Cahill *et al.* do not, and we have no explanation for this. We point out, however, that their interference filter had a FWHM bandpass of 0.8 nm, compared with our filter’s 0.14 nm bandpass, and that Fulcher-band transitions in the vicinity of 622–623 nm are spectrally dense [22]. Our rotationally unresolved data, taken with a 10 nm bandpass filter (Fig. 2), do not reach negative P_1 values, although they are certainly trending in this direction.

The cause of these negative values, and the basic physics underlying this novel threshold behavior, can be understood classically for the case of $Q(1)$ transitions with the help of Figs. 1(b) and 1(c). Unlike the atomic case, the

threshold restriction that the momentum transfer be along the z axis allows for either Π or Σ states with $M_N = 0$ or ± 1 to be excited. For the case of Π excitation, this can only happen when the target’s internuclear axis is perpendicular to z . When an excited Π state decays, it emits light with $P_1 \geq 0$ if $M_N = \pm 1$, and $P_1 \leq 0$ if $M_N = 0$; this is the opposite of the case for $P \rightarrow S$ atomic fluorescence. Thus, the negative sign of P_1 in our measurements at threshold indicates a slight dynamical preference for excitation of states with $M_N = 0$. This is somewhat surprising, given that the ground state ($N = 1$, $M_N = \pm 1$) sublevels are twice as common as those with $M_N = 0$, and can only be excited to Π states at threshold, whereas the $M_N = 0$ states can be excited to either Π or Σ states. This result also disagrees with the calculations of Meneses *et al.* [17], in which the excitation of Π states with $M_N = 0$ vanishes at threshold. We note, however, that the symmetry arguments of Dunn [23], invoked in Ref. [17], do not forbid $P_1 < 0$.

The nonzero P_3 values shown in Fig. 3(b), which are relatively insensitive to the incident beam energy, represent the observation of orientation for rotationally resolved molecular states. Earlier electron- H_2 601.8 nm photon coincidence experiments by McConkey *et al.* [15] attempted to observe a nonzero P_3 caused by the breakdown of axial collision symmetry, but their statistical accuracy was insufficient to achieve this goal. This illustrates the principle that sometimes angle-averaged experiments, while losing information related to specific momentum transfer, can provide new, related information because of their higher count rates. Finally, we note that, for a given rotationally resolved transition, the data of Figs. 2 and 3 are essentially independent of vibrational quantum number and isotopic composition.

We now attempt to explain the above observations more quantitatively using the formalism of state multipoles [5,6]. For unpolarized electrons, early work on this problem was carried out by Blum and Jakubowicz [24]. They showed that a nonzero P_1 can be measured due to the alignment created in the orbital angular momentum (electrons plus nuclei) N system. Over time, however, this initial alignment is decreased via fine-structure and hyperfine-structure depolarization due to coupling with the electronic (S) and nuclear (I) spins.

If spin-polarized electrons are used, the situation becomes more complicated. In the present case, the spin polarization of the electrons is transferred to the S system of the excited $^3\Pi_u$ state via electron exchange. From there, spin-orbit interactions lead to a partial transfer of this polarization to the N and I systems. The observed value of P_3 is ultimately due to the orientation of N .

Depolarization effects can be treated with the formalism of “generalized perturbation coefficients” using coupled state multipoles for three systems: N , S , and I [25,26]. In H_2 and D_2 , Hund’s case (b) coupling is a reasonable

starting point, since $N = \Lambda + R$ (where Λ is the projection of the electronic orbital angular momentum on the internuclear axis and R is the nuclear rotational angular momentum) is a good quantum number. In this scheme, $N + S \rightarrow J$ and $J + I \rightarrow F$. However, since J and F are not good quantum numbers for the $d^3\Pi_u$ state [27], one may ultimately need to consider other coupling schemes [6,24]. Note that relatively simple results can only be derived if all fine- and hyperfine-level splittings are large compared with the fluorescence linewidth γ . Since this is true in the present case, full depolarization of S occurs.

The time-averaged multipole moments of the excited molecular system are expressed as [25]

$$\overline{\langle T_{KQ}^+(N) \rangle} = \sum_{K'Q'k'q'} \langle T_{K'Q'}^+(N) \rangle \langle t_{k'q'}^+ \rangle G_{K'k'K}^{Q'q'Q}. \quad (1)$$

Here, $\langle T_{K'Q'}^+(N) \rangle$ and $\langle t_{k'q'}^+ \rangle$ are the initial state multipoles of the N and S systems, respectively, while the $G_{K'k'K}^{Q'q'Q}$ are the generalized perturbation coefficients. We absorb a factor $1/\sqrt{2I+1}$, i.e., the monopole term from the unpolarized nuclear system, into $G_{K'k'K}^{Q'q'Q}$ below. In addition to the monopole terms $\langle T_{00}^+(N) \rangle \langle t_{00}^+ \rangle$, the only parameters that enter the relevant equations for dipole radiation are the alignment $\langle T_{20}^+(N) \rangle$ and spin orientation $\langle t_{11}^+ \rangle = iP_e/3$ [28].

In our notation, and for our special case of an initially unpolarized nuclear spin system, the generalized perturbation coefficients are given by

$$G_{K'k'K}^{Q'q'Q} = \sqrt{\frac{(2K'+1)(2k'+1)(2K+1)}{(2S+1)(2I+1)^2}} \sum_J (-1)^{N-S-J-Q} \times (2J+1)^2 \begin{pmatrix} K' & k' & K \\ Q' & q' & -Q \end{pmatrix} \begin{Bmatrix} N & J & S \\ J & N & K \end{Bmatrix} \times \begin{Bmatrix} N & S & K \\ N & S & K \\ K' & k' & K \end{Bmatrix} \sum_F (2F+1)^2 \begin{Bmatrix} F & F & K \\ J & J & I \end{Bmatrix}. \quad (2)$$

We can now calculate P_1 and P_3 using Eqs. (4.6.10), (4.6.11), and (6.1.1) from Ref. [5]. All results can be expressed in terms of the relative alignment parameters $A_{20}(N) \equiv \overline{\langle T_{20}^+(N) \rangle} / \overline{\langle T_{00}^+(N) \rangle}$ and $A_{11} \equiv \overline{\langle t_{11}^+ \rangle} / \overline{\langle t_{00}^+ \rangle}$. For the various transitions considered here, we obtain

$$Q(1): P_1 = \frac{0.061A_{20}(1)}{1 + 0.020A_{20}(1)}, \quad (3)$$

$$R(1): P_1 = \frac{0.195A_{20}(2)}{1 - 0.065A_{20}(2)}, \quad (4)$$

$$Q(3): P_1 = \frac{0.321A_{20}(3)}{1 + 0.214A_{20}(3)}, \quad (5)$$

with

$$A_{20}(1) = \sqrt{2}(\sigma_1 - \sigma_0)/\sigma(N=1), \quad (6)$$

$$A_{20}(2) = \sqrt{10/7}(2\sigma_2 - \sigma_1 - \sigma_0)/\sigma(N=2), \quad (7)$$

$$A_{20}(3) = \sqrt{1/3}(5\sigma_3 - 3\sigma_1 - 2\sigma_0)/\sigma(N=3). \quad (8)$$

Here, $\sigma_m = \sigma_{-m}$ are magnetic sublevel cross sections, and σ is the angle-integrated cross section.

Consequently, the observable value of P_1 must lie between particular limits. The extreme cases occur when σ_0 or $\sigma_{m_{\max}}$ dominates the excitation process. The ranges are

$$Q(1): -8.9\% \leq P_1 \leq +4.3\%, \quad (9)$$

$$R(1): -21\% \leq P_1 \leq +25\%, \quad (10)$$

$$Q(3): -49\% \leq P_1 \leq +35\%. \quad (11)$$

The formula and the limit for the $Q(1)$ transition were also derived by Meneses *et al.* [17]. The small difference between our range and theirs is due to their (incorrect) value of $\bar{G}_0 = 0.964$ instead of 1. The energy dependence of their theoretical prediction for P_1 is due entirely to their dynamical calculation of the various σ_m .

In the formula for P_3 , A_{20} only appears in the denominator, i.e., in the expression for intensity. Our experimental results for P_1 show that the influence of the term with A_{20} is small, either because $|A_{20}|$ is small itself or, as for the $Q(1)$ transition, because strong depolarization results in a small perturbation coefficient.

With this assumption, the result for P_3 depends only on A_{11} . The latter parameter is constructed from $\overline{\langle T_{00}^+(N) \rangle}$, $\overline{\langle T_{20}^+(N) \rangle}$, and $\overline{\langle t_{11}^+ \rangle} = iP_e/3$. Since $G_{211}^{011} \ll G_{011}^{011}$ in all cases, the term with $\overline{\langle T_{20}^+(N) \rangle}$ can be neglected as well. Since the only remaining parameter that depends on the dynamics, $\overline{\langle T_{00}^+(N) \rangle}$, cancels out in the formula for the circular polarization, the circular polarization P_3 is directly proportional to the electron spin polarization, with the proportionality factor given by combinations of $3j$, $6j$, and $9j$ symbols. We obtain the following:

$$Q(1): P_3/P_e \approx -18.7\%, \quad (12)$$

$$R(1): P_3/P_e \approx -29.5\%, \quad (13)$$

$$Q(3): P_3/P_e \approx -5.3\%. \quad (14)$$

As seen in Fig. 3, the predictions for the $Q(N)$ transitions are in satisfactory agreement with the measurements. The $R(1)$ experimental results are, however, consistently below theory. We speculate that this is because the $d^3\Pi_u^+$ state, the parent for $R(1)$ fluorescence, is significantly perturbed by the $d^3\Sigma_u^+$ state [16,27]. This extra Σ character of the wave function should reduce its overall orientation. In general, we note again that neither J nor F is a good quantum number in the $d^3\Pi_u^+$ state. Thus, pure Hund's

case (b) coupling may need to be replaced in a more rigorous approach by an intermediate coupling scheme developed from a calculation of the molecular hyperfine dynamics [6,24,27].

In summary, the present data point out the qualitatively different physics between atoms and molecules in near-threshold excitation. We have observed a change near threshold in the sign of molecular fluorescence polarization (alignment) due to the dynamical energy dependence of the various magnetic substate cross sections, as opposed to variation caused by target coupling or resonance effects. Moreover, we have observed circularly polarized fluorescence polarization from rotationally and vibrationally resolved excited target states resulting from their orientation induced by exchange excitation with spin-polarized electrons. These measurements represent a systematic set of benchmark data for electron-molecule scattering, which will hopefully stimulate further theoretical development in the study of electron-molecule collisions.

We would like to thank Professor G. F. Hanne for helpful discussions. This work was supported by the NSF under Grants No. PHY-0855629 and No. PHY-1206067 (T. J. G.) and Grant No. PHY-1068140 (K. B.).

-
- [1] J. Franck and G. Hertz, *Verh. Dtsch. Phys. Ges.* **16**, 457 (1914).
 - [2] T. J. Gay, *Adv. At. Mol. Opt. Phys.* **57**, 157 (2009).
 - [3] N. Andersen and K. Bartschat, *Polarization, Alignment, and Orientation in Atomic Collisions* (Springer, New York, 2001).
 - [4] I. C. Percival and M. J. Seaton, *Phil. Trans. R. Soc. A* **251**, 113 (1958).
 - [5] K. Blum, *Density Matrix Theory and Applications* (Plenum, New York, 1996), 2nd ed.
 - [6] U. Fano and J. H. Macek, *Rev. Mod. Phys.* **45**, 553 (1973).
 - [7] C. Herting and G. F. Hanne, *J. Phys. B* **35**, L91 (2002).
 - [8] H. W. B. Skinner and E. T. S. Appleyard, *Proc. R. Soc. A* **117**, 224 (1927).
 - [9] V. Zeman, K. Bartschat, C. Norén, and J. W. McConkey, *Phys. Rev. A* **58**, 1275 (1998).
 - [10] See, e.g., R. H. McFarland, *Phys. Rev.* **133**, A986 (1964), and references therein.
 - [11] D. W. O. Heddle, *J. Phys. B* **16**, 275 (1983).
 - [12] S. J. Buckman and C. W. Clark, *Rev. Mod. Phys.* **66**, 539 (1994).
 - [13] P. Cahill, R. Schwartz, and A. N. Jette, *Phys. Rev. Lett.* **19**, 283 (1967).
 - [14] J. W. Maseberg and T. J. Gay, *Phys. Rev. A* **79**, 022705 (2009).
 - [15] J. W. McConkey, S. Trajmar, J. C. Nickel, and G. Csanak, *J. Phys. B* **19**, 2377 (1986).
 - [16] P. Baltayan and O. Nedelec, *J. Phys. (Paris)* **36**, 125 (1975).
 - [17] G. D. Meneses, L. M. Brescansin, M. T. Lee, S. E. Michelin, L. E. Machado, and G. Csanak, *Phys. Rev. A* **52**, 404 (1995).
 - [18] J. W. Maseberg and T. J. Gay, *J. Phys. Conf. Ser.* **212**, 012021 (2010).
 - [19] C. Mette and G. F. Hanne (private communication).
 - [20] D. H. Yu, J. F. Williams, X. J. Chen, P. A. Hayes, K. Bartschat, and V. Zeman, *Phys. Rev. A* **67**, 032707 (2003).
 - [21] A. Weingartshofer, E. M. Clarke, J. K. Holmes, and J. Wm. McGowan, *J. Phys. B* **8**, 1552 (1975), and references therein.
 - [22] A. Aguilar, J. M. Ajello, R. S. Mangina, G. K. James, H. Abgrall, and E. Roueff, *Astrophys. J. Suppl. Ser.* **177**, 388 (2008).
 - [23] G. H. Dunn, *Phys. Rev. Lett.* **8**, 62 (1962).
 - [24] K. Blum and H. Jakubowicz, *J. Phys. B* **11**, 909 (1978).
 - [25] K. Bartschat, H. J. Andrä, and K. Blum, *Z. Phys. A* **314**, 257 (1983).
 - [26] S. M. Khalid and H. Kleinpoppen, *Z. Phys. A* **311**, 57 (1983).
 - [27] T. A. Miller and R. S. Freund, *J. Chem. Phys.* **58**, 2345 (1973).
 - [28] K. Bartschat and K. Blum, *Z. Phys. A* **304**, 85 (1982).